
[View Journal Online](#)  
[View Article Online](#)

## Removal of methylene blue in aqueous solutions by electrocoagulation process: Adsorption and kinetics studies

Alain Stéphane Assémian <sup>1,2,\*</sup>, Konan Edmond Kouassi <sup>1,2</sup>, Kopoin Adouby <sup>1</sup>,  
 Patrick Drogui <sup>3</sup> and David Boa <sup>2</sup>

<sup>1</sup> Laboratoire des Procédés Industriels, de Synthèse de l'Environnement et des Energies Nouvelles (LAPISEN), Institut National Polytechnique Houphouët-Boigny, Yamoussoukro, 1313, Côte d'Ivoire

assmian07@yahoo.fr (A.S.A.), kouassikedmond@yahoo.fr (K.E.K.), adoubyk@yahoo.fr (K.A.), boadavidfr@yahoo.fr (D.B.)

<sup>2</sup> Laboratoire de Thermodynamique et de Physico-Chimie du Milieu (LTPCM), UFR-SFA, Université Nangui-Abrégoua, Abidjan, 801, Côte d'Ivoire

<sup>3</sup> Institut National de la Recherche Scientifique (INRS Eau Terre et Environnement), Université du Québec, 490 rue de la Couronne, Québec City, G1K9A9, Canada  
 patrick.drogui@ete.inrs.ca (P.D.)

\* Corresponding author at: Laboratoire des Procédés Industriels, de Synthèse de l'Environnement et des Energies Nouvelles (LAPISEN), Institut National Polytechnique Houphouët-Boigny, Yamoussoukro, 1313, Côte d'Ivoire.

Tel: +225.58970905 Fax: +225.30640406 e-mail: [assmian07@yahoo.fr](mailto:assmian07@yahoo.fr) (A.S. Assémian).

### RESEARCH ARTICLE



 10.5155/eurjchem.9.4.311-316.1736

Received: 19 May 2018

Received in revised form: 01 August 2018

Accepted: 03 August 2018

Published online: 31 December 2018

Printed: 31 December 2018

### KEYWORDS

Kinetic  
 Removal  
 Adsorption  
 Methylene blue  
 Electrocoagulation  
 Monopolar configuration

### ABSTRACT

The purpose of this study is to understand the mechanism driving the removal of methylene blue through electrocoagulation process. Experiments were carried out using iron as anode and cathode in a batch electrochemical cell operated in a monopolar configuration. The effects of operating parameters (initial pH, current density, initial dye concentration and energy consumption) on the removal of methylene blue from solution were investigated. The results showed that the optimum removal efficiency of 93.2% was achieved for a current density of 9.66 mA/cm<sup>2</sup>, optimal pH of 8±0.01 with a specific energy consumption of 7.451 kWh/m<sup>3</sup>. Afterwards, first and second-order rate equations were successively applied to study adsorption kinetics models. On top of usual correlation coefficients (*r*<sup>2</sup>), statistical test Chi-square ( $\chi^2$ ) were applied to evaluate goodness of fit and consequently find out the best kinetic model. Results showed that MB adsorption process onto iron hydroxides formed in aqueous solution during electrocoagulation treatment followed a second-order kinetic.

Cite this: *Eur. J. Chem.* **2018**, *9*(4), 311-316

Journal website: [www.eurjchem.com](http://www.eurjchem.com)

### 1. Introduction

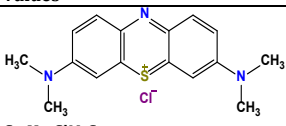
Accelerated development of industries activities didn't unfortunately happen without dramatic repercussions for the environment, in particular when they reject their wastewaters. Textile industries are among the major polluting industries in terms of discharged volume and characteristics [1]. Approximately 125-150 L of water are used for 1 kg of textile product [2]. Several studies have reported that there are more than 100,000 commercially available dyes with an estimated annual production of over 700,000 tons of dye-stuff [3,4]. Textile preparation, dyeing and finishing operations contribute to the complexity of the total effluent, making its treatment a rather difficult task. Moreover, depending on the particular dye class in use, the percentage of dye that remains unfixed to the fiber during the dyeing process, and finds its way into the effluent, can range from 5-50% [5,6].

Dye molecules comprise of two key components; the chromophores, responsible for producing the color, and the

auxochromes, which are not only supplement the chromophore but also render the molecule soluble in water and give enhanced affinity towards the fibers [7]. Due to their color content, dye bath effluents in particular, are not only aesthetic and undesirable pollutants, but may also interfere with light penetration in the receiving water bodies (impede photosynthesis). Thereby, the depletion of the dissolved oxygen occurs and the biological metabolism processes are upset.

Besides, dye-containing effluent is toxic to the environment since dyes are stable compounds, with low biodegradability and can be carcinogenic mutagenic, or teratogenic [8,9]. Dye removal by traditional treatment methods (biological process) is limited and inadequate since the majority of textile dyes possess complex aromatic molecular structures, which resist to biodegradation. Today, political authorities all over the world are aware of the necessity to protect the environment for a sustainable development and for future generations. Increasingly, strict legislation is being imposed on textile effluent discharge in order to be colorless. This is how limits

**Table 1.** Physicochemical properties of methylene blue.

Properties	Values
Molecular structure	
Chemical formula	C <sub>16</sub> H <sub>18</sub> ClN <sub>3</sub> S
IUPAC Name	3,7-Bis(Dimethylamino)phenazathionium chloride trihydrate
Molecular weight (g/mol)	319.85
Solubility (g/L)	50 (20 °C)
pK <sub>a</sub>	3.8
λ <sub>max</sub> (nm)	650
Class	Cationic dye
Name (CI)	Basic Blue 9 (BB9)
Colour Index (CI) number	52015

on color are imposed to industrial effluents before their reject in receiving surroundings [5,10]. Dyestuff and colored materials in wastewater can be effectively destroyed by advanced chemical oxidation such as ozonation, photocatalysis, fenton, electrooxidation (UV/H<sub>2</sub>O<sub>2</sub>, O<sub>3</sub>, O<sub>3</sub>/H<sub>2</sub>O<sub>2</sub>, UV/O<sub>3</sub>, UV/H<sub>2</sub>O<sub>2</sub>, H<sub>2</sub>O<sub>2</sub>/Fe<sup>2+</sup>), and adsorption using activated carbon (biosorption). In spite of the good oxidation of refractory organic compounds, the complexity of these methods (AOPs), high chemical consumption and relatively higher treatment cost constitute major barriers for field application purposes [11].

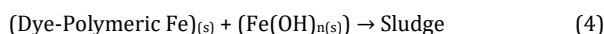
From that point of view, electrocoagulation (EC) process constitutes an interesting alternative because of its simplicity, short reaction time, low maintenance, low sludge production. Moreover, EC is easily operable, and there is no need to add systematically chemical substances as in coagulation-flocculation (CF) process for instance. It does not necessarily require addition of neither coagulant or flocculent, nor chemical storage and it efficiently removes colloidal particles [12]. A large amount of scientific researches on the treatment of textile wastewater by EC are available. However, they mainly focused on optimizing operating parameters (pH, current density, initial concentration, connection mode (MP/BP), electrode type (Fe, Al), inter-electrode distance, electrolysis time, agitation speed etc.). So, only a few researches have tried to delineate the EC mechanism [13]. Indeed, an examination of the available literature reveals that EC mechanism and particularly the determination of suitable kinetic model, is still incompletely explored [11,14].

Electrocoagulation can be defined as an emerging technology used for treatment of various industries wastewater owing to its *in-situ* generation of coagulating agents by electro-oxidation of "sacrificial anodes". It is generally accepted that EC process involves three successive stages: (a) formation of coagulants by electrolytic oxidation of the "sacrificial electrode"; (b) aggregation of the destabilized phases to form flocs; (c) destabilization of the contaminants, particulate suspension, and breaking of emulsions [13,15]. Freshly formed amorphous «sweep flocs» (Fe(OH)<sub>3(s)</sub>) have large surface areas, which is beneficial for a rapid adsorption of soluble organic compounds and trapping colloidal particles [16]. These insoluble metal hydroxides (Fe(OH)<sub>3(s)</sub>) can remove dye molecules dissolved in the solution by surface complexation, adsorption or electrostatic attraction [17]. In surface complexation, it is assumed that the pollutant can act as a ligand to bond with a hydrous iron moiety following precipitation and adsorption mechanisms [18,19].

Precipitation:



Adsorption:



The global purpose of this study is to investigate at laboratory scale mechanism which leads to the removal of a basic synthetic dye, methylene blue (MB), selected as the model pollutant. The following study occurs in two steps: (i) Evaluate firstly the effect of pH, current density and initial concentration on MB removal by EC process; (ii) Secondly, determine the suitable kinetic model between pseudo first-order and pseudo second-order.

## 2. Experimental

### 2.1. Preparation of the synthetic solution

All solutions used for electrolysis tests were prepared from analytical grade chemicals reagents with distilled water. Methylene blue especially due to its chemical stability and its use in textile industry was selected as pollutant model. His physical and chemical properties are shown in Table 1. MB was purchased from Merck (Germany, purity 99 %). Synthetic solution stock was freshly prepared before set of experiments by dissolving the exact MB amount in distilled water. A fixed amount of sodium sulphate 0.2 g/L (Na<sub>2</sub>SO<sub>4</sub>; Prolabo; purity 99%) was added as a supporting electrolyte to increase the conductivity.

The pH of the untreated solution was adjusted to the desired value using either 1.0 N HCl (Panreac, purity 37%) or sodium hydroxide pellets 1.0 N NaOH (Panreac, purity 98%). At the end of each test, the reactor content was decanted in a test-tube of 2 L capacity. Then, the supernatant was filtered on Büchner on which was put a 1.5 µm glass microfiber filter Whatman™. Finally, the residual concentration of MB collected from the filtrate was determined by using a UV-Vis spectrophotometer (JASCO UV-530, Japan) at the maximum absorbance characteristic of MB (λ<sub>max</sub> = 650 nm). The MB removal rate R (%) was calculated using the Equation (5).

$$R(\%) = \frac{C_0 - C_f}{C_0} \times 100 \quad (5)$$

where C<sub>0</sub> and C<sub>f</sub> represent respectively the initial and final dye concentration.

### 2.2. Electrocoagulation reactor set-up

Runs were performed with a working volume of 1.7 L at room temperature in batch mode. The EC reactor cell was made in transparent Plexiglas with parallelepiped shape dimensions: 125 mm (length) × 125 mm (width) × 200 mm

(height) and was equipped with ten electrodes connected in monopolar parallel (MPP) configuration. These iron electrodes (five cathodes and five anodes) with the dimension of 11 mm (length) × 10 mm (width) × 1 mm (thickness), made of iron plate were installed vertically and alternately on a Plexiglas support with an electrode gap of  $e = 10$  mm. Each electrode has an active surface area of 110 cm<sup>2</sup>. The Plexiglas support was maintained at 20 mm from the bottom of the EC reactor. The desired current intensity was delivered by means of DC power supply (ELC-AL781D: 0-5 A; 0-30 V, France) under potentiostatic operational conditions.

Before each run both electrodes (anodes and cathodes) were washed with sponge prior immersed in HCl (0.1 N) during 20 minutes in order to remove compounds deposited on the electrodes surface, then rinsed with tap water, dried in an oven at 105 °C for 20 minutes, and weighted. A magnetic stirrer (Heidolph Drehzahl, Germany) continuously mixed the synthetic solution to assure constant homogeneity. The mixture was monitored to avoid flocks destruction freshly formed during the treatment. An electronic pH-meter (Hanna HI 8424, USA) was used to measure pH variation. The operation started when the current density was adjusted to a desired value and stopped with the power generator turned off.

### 2.3. Adsorption kinetics modeling

In order to investigate the adsorption process kinetics, two different kinetic models among the most used in the literature were applied to analyze the kinetics of MB removal. These are respectively first and second order Lagergren models.

#### 2.3.1. First-order Lagergren model

The first order Lagergren model is generally expressed as follows [20,21]:

$$\frac{dq_t}{dt} = k_1 (q_e - q_t) \quad (6)$$

where  $q_e$  (mg/g) and  $q_t$  (mg/g) are, respectively, the adsorption capacities at equilibrium and at any time  $t$  (min).  $k_1$  (min<sup>-1</sup>) in this equation is a first order adsorption rate constant. The integrated form of the above equation with the boundary conditions  $t = 0$  to  $t = t$  and  $q_t = 0$  to  $q_t = q_t$  is rearranged to obtain the following time dependent function:

$$\text{Log}(q_e - q_t) = \text{Log}(q_e) - t_1 / 2.303 \quad (7)$$

#### 2.3.2 Second-order Lagergren model

The Lagergren second-order kinetic model is generally expressed as [20,21]:

$$dq/dt = k_2 (q_e - q_t)^2 \quad (8)$$

where  $k_2$  is the second-order adsorption rate constant. After integration of the previous equation with the boundary condition  $t = 0$ ,  $t_0 > 0$  ( $q = 0$  to  $>0$ ), we got the following:

$$1/(q_e - q_t) = 1/q_e \quad (9)$$

This equation can be rearranged and linearized as [22]:

$$t/q_t = 1/k_2 q_e^2 + t/q_e \quad (10)$$

In this mathematical shape  $q_e$  and  $q_t$  are, respectively, the amount of MB adsorbed on iron hydroxides (mg/g) at equilibrium and at any time  $t$  (min).  $k_2$  is the rate constant of the second order kinetic model.  $q_e$  (cal), the equilibrium adsorption capacity and  $k_2$ , were determined from the slope and intercept of the plot  $t/q_t$  versus time ( $t$ ).

### 2.4 Statistical test for the kinetics data

The analysis of the correlation coefficients does not always make it possible to identify directly the theoretical model approaching the experimental data. In this case, the application of statistical criteria such as Chi-square ( $\chi^2$ ) or sum of error squares (SSE) for instance is necessary for valid and reliable conclusions. In this study, the suitability and accuracy of both pseudo-first-order and pseudo-second-order kinetic models were evaluated using the Chi-square ( $\chi^2$ ) represented as follows:

$$\chi^2 = (q_e^{exp} - q_e^{cal})^2 / q_e^{cal} \quad (11)$$

where  $q_e$  (exp) is the experimental equilibrium adsorption capacity (mg/g), and  $q_e$  (cal) is the calculated equilibrium adsorption capacity (mg/g).  $\chi^2$  measures the goodness of fit between the experimental and calculated equilibrium adsorption capacity. The value of  $\chi^2$  for the suitable model should be the lowest. A high correlation coefficient ( $r^2$ ) with a low value of Chi-square ( $\chi^2$ ) indicate that the model is applicable.

## 3. Results and discussion

### 3.1. The current density effect

Current density applied during electrocoagulation process is recognized to be one of the main operating parameter that strongly affects anodic dissolution [16,23]. So, the amount of MB removal depends on adsorbent dose and the bubbles (H<sub>2</sub>; O<sub>2</sub>) generated in the electrochemical cell. To measure the impact of current density on the electrocoagulation process a set of experiments was carried out using synthetic solutions containing an initial concentration of 50 mg/L of MB at a pH 8.0±0.01, with the current density varying from 1.45 to 14.5 mA/cm<sup>2</sup>. The results show that the removal efficiency increased with the increase of current density and reached a maximum rate of MB removal (84.79%) and then decreased slowly (Figure 1). These results were consistent with those recorded by Adeogun during the treatment of Rhodamine B (RhB) by using EC process [14].

This could be attributed to the increase of iron coagulant generated *in-situ* by anode electrodisolution, thereby resulting in rapid removal of MB. Besides, according to Faraday's law, the current density is directly proportional to the amount of adsorbent (iron hydroxides) generated [18]. Hence, the amount of dye adsorption increased with the increase in adsorbent concentration in the reactor. This could indicate that the adsorption depends upon the availability of binding sites for iron.

Based on Faraday's law the energy consumed is proportional to the current density applied during the electrolytic process. As can be seen in Figure 1, this energy consumed increases with the increase of current density. So, additional experiments were carried out at 9.66 mA/cm<sup>2</sup> corresponding to a specific energy consumption of 7.451 kWh/m<sup>3</sup>.

### 3.2. The pH effects

EC performance can be also influenced by characteristics of the aqueous medium, especially pH of the electrolyte [15,20-22,24].

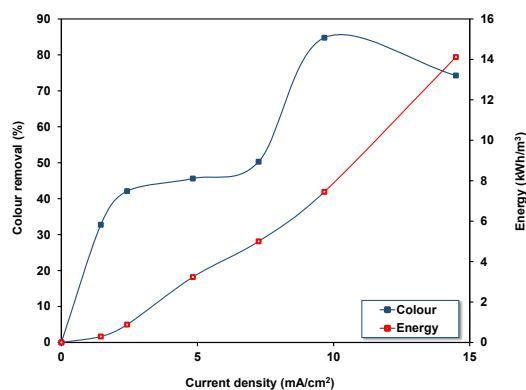


Figure 1. Effect of current density on methylene blue removal (pH = 8;  $C_0 = 50$  mg/L).

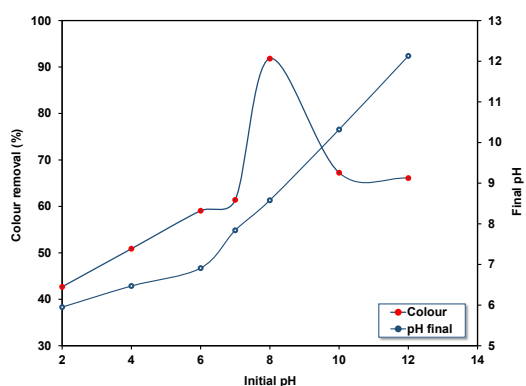


Figure 2. Effect of initial pH on methylene blue removal (pH = 8;  $C_0 = 50$  mg/L;  $J = 9.66$  mA/cm<sup>2</sup>).

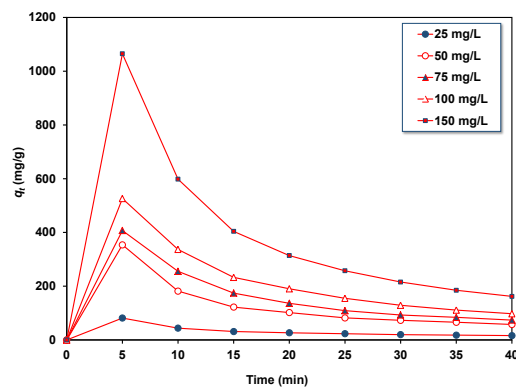


Figure 3. Effect of initial concentration on methylene blue removal (pH = 8;  $J = 9.66$  mA/cm<sup>2</sup>).

A set of experiments were carried out by ranging initial pH between 2 and 12. The evolution of MB removal as a function of the initial pH is depicted in Figure 2. The analysis of this graph reveals that the removal efficiency increased with initial pH until a maximum of 91.81% corresponding to an initial pH of  $8 \pm 0.01$  and then decreased describing a curve shape in bell. Several investigators have also observed similar trend of maximum removal efficiency close to this initial pH value [14, 25,26]. Iron generated during electrolysis can be in different forms (monomeric ions and polymeric hydroxyl complex):  $\text{Fe}(\text{H}_2\text{O})_6^{3+}$ ,  $\text{Fe}(\text{H}_2\text{O})_5^{2+}$ ,  $\text{Fe}(\text{H}_2\text{O})_4(\text{OH})^{2+}$ ,  $\text{Fe}(\text{H}_2\text{O})_3(\text{OH})_2^{4+}$  and  $\text{Fe}_2(\text{H}_2\text{O})_6(\text{OH})_4^{4+}$  depending upon the pH of the aqueous medium that finally transform into insoluble species  $\text{Fe}(\text{OH})_3$  according to complex precipitation [13].

Otherwise,  $\text{Fe}(\text{OH})_3$  also called bernalite is reported to be the predominant specie present in solution according to Fe-

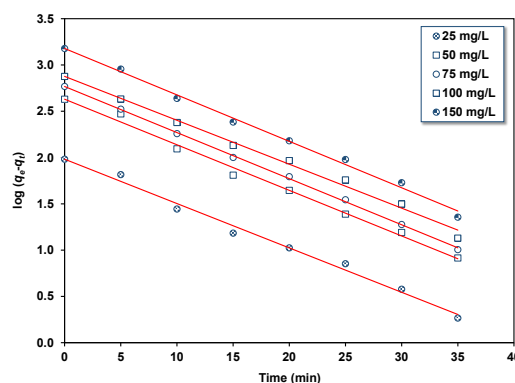
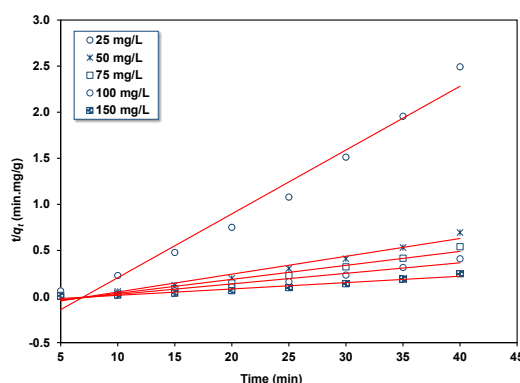
$\text{H}_2\text{O}$  Pourbaix diagram. Freshly formed amorphous  $\text{Fe}(\text{OH})_3$  or «sweep flocs» have large surface areas which are beneficial for a rapid adsorption of soluble organic compounds like dyes and trapping of colloidal particles [16]. These species are probably responsible of methylene blue removal by adsorption phenomenon.

### 3.3. The initial dye concentration effect

The effect of initial dye concentration on methylene blue removal was shown in Figure 3. For dye concentrations increasing from 25 to 150 mg/L the process showed high removal in the first five min for all the concentrations studied. These peaks earlier observed in this graph could be assigned to available sites on amorphous iron hydroxides precipitates  $\text{Fe}(\text{OH})_3$  freshly formed in the medium and not yet occupied.

**Table 2.** Adsorption constants for first and second order kinetic model.

$C_0$ (mg/L)	$q_e^{exp}$ (mg/g)	Pseudo-first order kinetic model				Pseudo-second order kinetic model			
		$q_e^{cal}$ (mg/g)	$k_1$ (min <sup>-1</sup> )	$\chi^2$	$r^2$	$q_e^{cal}$ (mg/g)	$k_2$ (mg/g.min)	$\chi^2$	$r^2$
25	16.0513	95.9842	0.1103	66.5658	0.9862	14.4509	-0.0098	0.1773	0.9719
50	57.5499	427.0709	0.1135	319.7263	0.9896	51.8135	-0.0026	0.6351	0.9688
75	73.9927	586.0032	0.1146	447.3606	0.9989	65.7895	-0.0020	1.0229	0.9644
100	97.4824	753.1821	0.1094	570.8341	0.9892	87.7193	-0.0014	1.0866	0.9534
150	162.0792	1508.3426	0.1156	1201.6003	0.9919	144.9275	-0.0008	2.0298	0.9543

**Figure 4.** Pseudo first order adsorption kinetic model of methylene blue removal.**Figure 5.** Pseudo-second order adsorption kinetic model of methylene blue removal at different concentrations.

The efficiency of the process increased from 25.1 to 134.3 mg/g as the initial concentration increased. After a retention time of 40 minutes, there was no significant difference noticed in the amount coagulated of the process. Consequently, a steady-state approximation was assumed and equilibrium situation was reached [14].

### 3.4. Kinetics modeling

#### 3.4.1. First-order Lagergren model

The experimental data were initially analyzed using the first order Lagergren model. The plot of  $\log(q_e - q_t)$  versus  $t$  should give the linear relationship from which  $k_1$  and  $q_e$  can be determined from the slope and intercept respectively (Figure 4). The computed results are presented in Table 1. Analysis of these results shows that the theoretical  $q_e$  (cal) value doesn't match with the experimental  $q_e$  (exp) values for all concentrations. Indeed, weak values of Chi-square ( $\chi^2$ ) obtained for statistical criterion selected is necessary to check the model validity. Therefore, this statistical condition should be rigorously observed before opting for this model. In our case, high value of Chi-square ( $\chi^2$ ) calculated clearly confirm a poor fit for first-order although high correlation coefficient ( $r^2$ ) are noticed. Therefore, this model is probably not the most appropriate for describing the kinetics of MB removal. The

experimental data were further fit with second order Lagergren model.

#### 3.4.2. Second-order Lagergren model

The corresponding data are presented in Table 2. The plots were found to be linear with good correlation coefficients (0.9719, 0.9688, 0.9644, 0.9534 and 0.9543 for 25, 50, 75, 100, and 150 mg/L initial dye concentration, respectively). Theoretical values  $q_e$  (cal) are a good match with the experimental  $q_e$  (exp) data for all concentrations studied compared to first order Lagergren model. Besides, a high correlation coefficient ( $r^2$ ) value conjugated to a low value of the Chi-square ( $\chi^2$ ) confirms a good fit for second order model.

### 3.5. Determination of kinetic model for MB removal

The calculation of the regression coefficient ( $r^2$ ) for pseudo-first and pseudo-second order are relatively close to 1 (Table 2). So, to determine the best model, a supplementary statistical test ( $\chi^2$ ) has been applied. According to Table 2, pseudo second-order shows high regression coefficient ( $r^2$ ) with a low value of  $\chi^2$  for each concentration studied while a rather high value of  $\chi^2$  is observed for the pseudo-first order model. It means that the kinetic of MB removal obeys to pseudo second-order. Similar results have been reported

previously by several authors while determining the most suitable kinetic model for 1-phenylazo-2-naphthol (PAN), alizarin saphirol (AS), indigo carmine (IC) [1,27-30]. On the other hand, other researchers determined the pseudo-first order as a suitable model to describe the kinetics for the following dyes: Rhodamine B (RhB), alizarin red S (ARS), methyl orange (MO), congo red (CR), methylene blue (BM-ylene), methyl blue (BM-yl) [14,20,27,29,31-34].

#### 4. Conclusion

This study aimed to explain removal mechanism occurring through electrocoagulation process applies to remove methylene blue. The treatment of this synthetic dye has been led in batch reactor with monopolar parallel connection. Results obtained show us that the process is greatly influenced by initial pH imposed. Indeed, we have found an optimal pH value of  $8 \pm 0.01$  corresponding to the predominance of  $\text{Fe}(\text{OH})_3$  specie. Optimal current intensity was found to be  $9.66 \text{ mA/cm}^2$  corresponding to a specific energy consumption of  $7.451 \text{ kWh/m}^3$ . The kinetic model after statistical tests could be quite successfully fitted by a pseudo-second order. Even though this work has allowed us to determine kinetic for MB removal, supplementary investigations such as isotherm adsorption and thermodynamic studies are necessary to better understand the complex mechanism leading to dyes removal by electrocoagulation process.

#### Acknowledgements

The authors are thankful to Institut National Polytechnique Houphouët-Boigny, Yamoussoukro, Côte d'Ivoire for their support.

#### Disclosure statement

Conflict of interests: The authors declare that they have no conflict of interest.

Author contributions: All authors contributed equally to this work.

Ethical approval: All ethical guidelines have been adhered.

#### ORCID

Alain Stéphane Assémian

 <http://orcid.org/0000-0001-7755-9775>

Konan Edmond Kouassi

 <http://orcid.org/0000-0002-1243-5330>

Kopoin Adouby

 <http://orcid.org/0000-0002-8015-2893>

Patrick Drogui

 <http://orcid.org/0000-0002-3802-2729>

David Boa

 <http://orcid.org/0000-0002-9804-5965>

#### References

- [1]. Kabdashi, I.; Arslan-Alaton, I.; Olmez-Hanci, T.; Tunay, O. *Environ. Technol. Rev.* **2012**, *1*, 2-45.
- [2]. Korbahiti, B. K.; Tanyolac, A. J. *Hazard. Mater.* **2008**, *151*, 422-431.
- [3]. Brillas, E.; Martínez-Huitle, C. A. *Appl. Catal. B Environ.* **2015**, *166*, 603-643.
- [4]. Robinson, T.; McMullan, G.; Marchant, R.; Nigam, P. *Bioresour. Technol.* **2001**, *77*, 247-255.
- [5]. Khandegar, V.; Saroha, A. K. *J. Environ. Manage.* **2013**, *128*, 949-963.
- [6]. Zidane, F.; Drogui, P.; Lekhlif, B.; Bensaid, J.; Blais, J. F.; Belcadi, S. *J. Hazard. Mater.* **2008**, *155*, 153-163.
- [7]. Gupta, V. K.; Suhas, null. *J. Environ. Manage.* **2009**, *90*, 2313-2342.
- [8]. Golder, A. K.; Hridaya, N.; Samanta, A. N.; Ray, S. J. *Hazard. Mater.* **2005**, *127*, 134-140.
- [9]. Merzouk, B.; Madani, K.; Sekki, A. *Desalination.* **2010**, *250*, 573-577.
- [10]. Alinsafi, A.; Khemis, M.; Pons, M. N.; Leclerc, J. P.; Yaacoubi, A.; Benhammou, A.; Nejmeddine, A. *Chem. Eng. Process. Intensif.* **2005**, *44*, 461-470.
- [11]. Zaviska, F.; Drogui, P.; Blais, J. F.; Mercier, G.; Lafrance, P. J. *Hazard. Mater.* **2011**, *185*, 1499-1507.
- [12]. Garg, K. K.; Prasad, B. *J. Environ. Chem. Eng.* **2016**, *4*, 178-190.
- [13]. Mollah, M. Y.; Morkovsky, P.; Gomes, J. A.; Kesmez, M.; Parga, J.; Cocke, D. L. *J. Hazard. Mater.* **2004**, *114*, 199-210.
- [14]. Adeogun, A. I.; Balakrishnan, R. B. *Appl. Water Sci.* **2017**, *7*, 1711-1723.
- [15]. Bazrafshan, E.; Moein, H.; Kord Mostafapour, F.; Nakhaie, S. *J. Chem.* **2012**, *2013*, 1-8.
- [16]. Drogui, P.; Blais, J. F.; Mercier, G. *Recent Patents Eng.* **2007**, *1*, 257-272.
- [17]. Kobya, M.; Can, O. T.; Bayramoglu, M. *J. Hazard. Mater.* **2003**, *100*, 163-178.
- [18]. Daneshvar, N.; Oladegaragoze, A.; Djafarzadeh, N. *J. Hazard. Mater.* **2006**, *129*, 116-122.
- [19]. Holt, P. K.; Barton, G. W.; Mitchell, C. A. *Chemosphere.* **2005**, *59*, 355-367.
- [20]. Nariyan, E.; Sillanpaa, M.; Wolkersdorfer, C. *Sep. Purif. Technol.* **2017**, *177*, 363-373.
- [21]. Majidi, M. R.; Danaee, I.; Nikmanesh, S. *Bulg. Chem. Commun.* **2016**, *48*, 628-635.
- [22]. Nongbe, M. C.; Bretel, G.; Ekou, T.; Ekou, L.; Yao, K. B.; Grogne, E.; Felpin, F. *Cellulose* **2018**, *25*, 4043-4055.
- [23]. Vasudevan, S.; Lakshmi, J. *Environ. Eng. Sci.* **2012**, *29*, 563-572.
- [24]. Chen, X.; Chen, G.; Yue, P. L. *Sep. Purif. Technol.* **2000**, *19*, 65-76.
- [25]. Tir, M.; Moulai-Mostefa, N. *J. Hazard. Mater.* **2008**, *158*, 107-115.
- [26]. Pajootan, E.; Arami, M.; Mahmoodi, N. M. *J. Taiwan Inst. Chem. E.* **2012**, *43*, 282-290.
- [27]. Mohammadlou, N.; Rasoulifard, M. H.; Vahedpour, M.; Eskandarian, M. R. *J. Appl. Chem. Res.* **2014**, *4*, 123-142.
- [28]. Ho, Y. S. *J. Hazard. Mater.* **2006**, *136*, 681-689.
- [29]. Miron, A. R.; Rikabi, A. K. K.; Niculae, A. G.; Tanczos, S. K. *Rev. Chim. Buchar.* **2015**, *66*, 6-12.
- [30]. Mkpennie, V. N.; Abakedi, O. U. *Curr. Res. Chem.* **2015**, *7*, 34-43.
- [31]. Song, P.; Yang, Z.; Zeng, G.; Yang, X.; Xu, H.; Huang, J.; Wang, L. *Water Air Soil Poll.* **2015**, *226*, 1-12.
- [32]. Kamaraj, R.; Ganesan P.; Vasudevan, S. *J. Electrochem. Sci. Eng.* **2014**, *4(4)*, 187-201.
- [33]. Samide, A.; Tutunaru, B.; Tigae, C.; Efreem, R.; Moanta, A.; Dragoi, M. *Environ. Prot. Eng.* **2014**, *40*, 93-104.
- [34]. Adeogun, A. I.; Balakrishnan, R. B. *J. Electrochem. Sci. Eng.* **2016**, *6*, 199-213.



Copyright © 2018 by Authors. This work is published and licensed by Atlanta Publishing House LLC, Atlanta, GA, USA. The full terms of this license are available at <http://www.eurjchem.com/index.php/eurjchem/pages/view/terms> and incorporate the Creative Commons Attribution-NonCommercial (CC BY NC) (International, v4.0) License (<http://creativecommons.org/licenses/by-nc/4.0>). By accessing the work, you hereby accept the Terms. This is an open access article distributed under the terms and conditions of the CC BY NC License, which permits unrestricted non-commercial use, distribution, and reproduction in any medium, provided the original work is properly cited without any further permission from Atlanta Publishing House LLC (European Journal of Chemistry). No use, distribution or reproduction is permitted which does not comply with these terms. Permissions for commercial use of this work beyond the scope of the License (<http://www.eurjchem.com/index.php/eurjchem/pages/view/terms>) are administered by Atlanta Publishing House LLC (European Journal of Chemistry).